ACS APPLIED MATERIALS & INTERFACES
Research Article
www.acsami.org

Degradation of Organic/Organic Interfaces in Organic Light-Emitting Devices due to Polaron–Exciton Interactions

Qi Wang and Hany Aziz*

Department of Electrical & Computer Engineering, and Waterloo Institute for Nanotechnology, University of Waterloo, 200 University Avenue West, Waterloo, Ontario, N2L 3G1, Canada

ABSTRACT: We study the stability of common hole transport material/electron transport material (HTM/ETM) interfaces present in typical organic light-emitting devices (OLEDs) under various stress scenarios. We determined that these interfaces degrade rapidly, because of an interaction between HTM positive polarons and HTM singlet excitons. The phenomenon results in a deterioration in conduction across the interface, and contributes to the commonly observed increase in OLED driving voltage with electrical driving time. This interfacial degradation can be slowed if the exciton lifetime becomes shorter. The findings uncover a new degradation mechanism that is interfacial in nature, which affects organic/organic interfaces in OLEDs and contributes to their limited electroluminescence stability, and shed light on approaches for reducing it. Although this study has focused on OLEDs, we can expect the same degradation mechanism to affect organic/organic interfaces in other organic optoelectronic devices where both excitons and polarons are present in high concentrations, such as in organic solar cells or photodetectors.

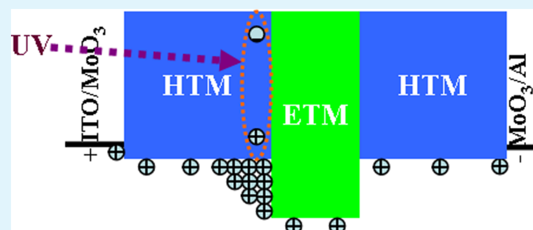

KEYWORDS: *organic/organic interface, interfacial degradation, OLED, polaron–exciton interaction, interfacial stability*

1. INTRODUCTION

The relatively short lifetime remains a critical issue for organic light-emitting devices (OLEDs), especially the most efficient ones.[1] Increasing the electroluminescence (EL) stability of OLEDs requires a fundamental understanding of the underlying degradation mechanisms. The issue has been the focus of a significant number of studies.[2−9] For example, we determined that the formation of unstable cationic and anionic species of the emitter materials plays a role in the degradation of fluorescent OLEDs.[3,4] Kondakov et al. identified the homolytic cleavage of C–N bonds in hole transport materials such as *N*,*N*′-bis(naphthalen-1-yl)-*N*,*N*′-bis(phenyl)benzidine (NPB)[5,6] and 4,4′-bis(*N*-carbazolyl)biphenyl (CBP)[7] when in singlet excited states as another degradation mechanism. Giebink et al. determined that annihilation reactions between host anions and guest excitons contribute to the degradation of phosphorescent OLEDs.[8,9] Despite their success in identifying several important degradation mechanisms in OLEDs, these studies have focused on degradation phenomena that occur in the organic materials bulk. Interfacial degradation, such as the interface between hole transport material (HTM) and electron transport material (ETM), where most electron–hole (e-h) recombination occurs and EL originates in an OLED, has never been systematically investigated.

Only a few studies have drawn the attention of EL degradation to the vicinity of HTM/ETM interfaces.[10−13] For instance, Scholz et al. identified possible chemical reactions of phosphorescent emitters with adjacent hole-blocking ETMs as the cause for EL degradation using laser desorption/ionization time-of-flight mass spectrometry.[10] Siboni et al. uncovered the role of the buildup of hole space charges in the vicinity of HTM/ETM interface in OLEDs degradation.[11−13] These studies have particularly emphasized the importance of the hole-blocking nature of ETMs in device EL degradation; however, the role of HTMs (or host materials in case of phosphorescent OLEDs) at HTM/ETM interfaces in device EL degradation has been overlooked. Moreover, the fundamental underlying mechanisms responsible for the degradation behaviors in these studies remain unclear.

We recently found that organic/electrode interfaces in OLEDs and other organic optoelectronic devices are extremely susceptible to degradation by excitions. This interfacial degradation is found to be photochemical in nature and results in a deterioration in charge injection.[14−17] Considering the extremely high density of excitons at HTM/ETM interfaces in an OLED during operation, it is natural to wonder if similar exciton-induced interfacial degradation occurs at these interfaces, and whether it plays a role in device overall degradation behavior. Furthermore, given the fact that HTM/ETM interfaces in operating OLEDs are also the places where high density of charge carriers (i.e., mostly hole carriers) is accumulated due to orders of magnitude differences in charge carrier mobility between HTMs and ETMs, it becomes interesting to wonder if these two species at the interfaces interact with each other and contribute to HTM/ETM interfacial degradation.

Received: June 28, 2013
Accepted: August 12, 2013
Published: August 12, 2013

 © 2013 American Chemical Society

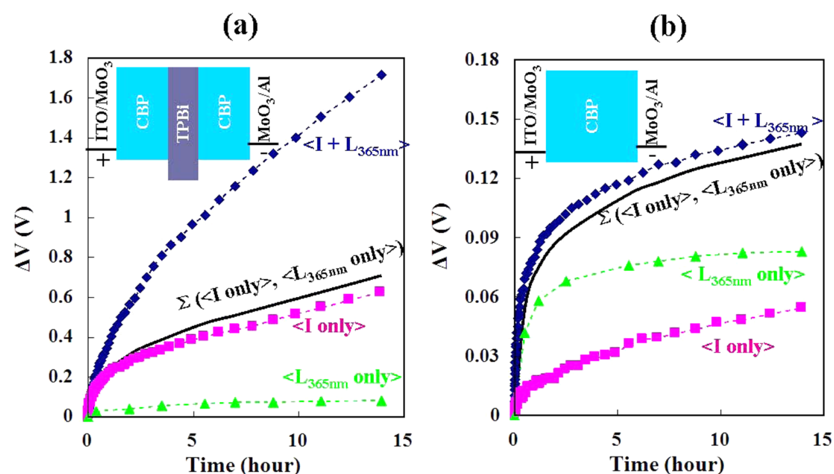

Figure 1. Change in driving voltage (ΔV) at 20 mA/cm^2 in devices (a) with and (b) without the TPBi layer, versus time, during which the devices are subjected to stress scenarios: ⟨I only⟩, ⟨$L_{365\text{ nm}}$ only⟩, and ⟨I + $L_{365\text{ nm}}$⟩. The curve $\sum$(⟨I only⟩, ⟨$L_{365\text{ nm}}$ only⟩) represents the algebraic sum of the ΔV values in ⟨I only⟩ and ⟨$L_{365\text{ nm}}$ only⟩.

In this study, we investigate the stability of HTM/ETM interfaces widely used in OLEDs, using, for this purpose, unipolar (hole-only) devices that are subjected to external illumination and/or current flow in order to study the effects of excitons and charges separately and also when they are both present. However, this is difficult to implement in actual OLEDs, because of the fact that subjecting OLEDs to current flow only inevitably leads to the creation of excitons and, thus, a scenario where both excitons and charges co-exist. Different from previous studies, this is the first work that investigates the effect of excitons and their possible interactions with charge carriers on organic/organic interfaces in OLEDs. In this work, CBP/1,3,5-tris(*N*-phenyl-benzimidazol-2-yl)-benzene (TPBi) and NPB/tris(8-hydroxyquinolinato)aluminum (AlQ_3) interfaces are studied as representative HTM/ETM interfaces, because of their widespread use in phosphorescent and fluorescent OLEDs, respectively. The results show that the HTM/ETM interfaces degrade significantly when subjected to light and current flow simultaneously. The degradation is found to be induced by interactions between HTM positive polarons and HTM singlet excitons in the vicinity of HTM/ETM interfaces. Reducing these interactions, for example, by means of reducing exciton lifetime, is found to reduce the interfacial degradation.

2. EXPERIMENTAL SECTION

In this work, devices utilizing archetypical organic materials are fabricated and tested. In these devices, NPB and CBP are used as HTMs, and AlQ_3 and TPBi are used as ETMs. Indium tin oxide (ITO) and aluminum (Al) are used as anode and cathode, respectively. All devices are fabricated by the deposition of the organic materials and metals at a rate of 1 Å/s using thermal evaporation in vacuum at a base pressure of $\sim 5 \times 10^{-6}$ Torr on CF_4/O_2 plasma-cleaned[16] ITO-coated glass substrates. Monochromatic illumination from a 200 W Hg−Xe lamp equipped with Oriel-77200 monochromator is used for irradiation tests. An Edinburgh Instruments Model FL920 spectrometer is used for time domain fluorescence lifetime measurements. All tests are carried out in a nitrogen atmosphere.

3. RESULTS AND DISCUSSION

We first study the stability of the CBP/TPBi interface under various stress scenarios. For this purpose, we utilize CBP hole-only (h-only) devices that contain a thin TPBi layer (~5 nm), and thus a CBP/TPBi interface, and others without the TPBi layer, for comparison. The structure of the devices is indium tin oxide (ITO)(120 nm)/MoO_3(5 nm)/CBP(20 nm)/TPBi(5 nm or 0 nm)/CBP(20 nm)/MoO_3(5 nm)/Al(100 nm). When under a forward bias (i.e., ITO is positively biased relative to Al), the 5-nm MoO_3 on the ITO side facilitates hole injection from ITO to CBP and the 5-nm MoO_3 on the Al side prevents electron injection from Al to CBP. Given the high hole mobility of CBP,[18] these devices show h-only transport characteristics. Since these devices do not emit light, we use changes in driving voltage (V_d) as an indicator of device degradation due to the different stress conditions.[15,16] Figures 1a and 1b show the changes in V_d (ΔV), defined as the V_d value at any given time needed to drive a current with a density of 20 mA/cm^2 minus the initial V_d value (at time = 0) in the devices with and without the TPBi layer, respectively, as a function of time, during which these devices are subjected to one of the following stress scenarios:

(1) current flow only (denoted by ⟨I only⟩), under a forward bias to sustain a current flow of density ~20 mA/cm^2;
(2) irradiation by light only (denoted by ⟨$L_{365\text{ nm}}$ only⟩), at 365 nm, with a power density of ~0.5 mW/cm^2; and
(3) current flow and irradiation together (denoted by ⟨I + $L_{365\text{ nm}}$⟩), in which the device is subjected to conditions (1) and (2) simultaneously.

As CBP absorbs significantly at 365 nm whereas TPBi does not,[9,15] this irradiation wavelength allows exciting CBP only, creating CBP singlet excitons. The initial V_d value of the devices with and without the TPBi layer (i.e., for the trends in Figures 1a and 1b, respectively) is ~5.5 V and ~1.3 V, respectively. As the figures show, subjecting both types of devices to light alone (i.e., ⟨$L_{365\text{ nm}}$ only⟩) for 14 h results in a small increase in V_d ($\Delta V \approx 0.08$ V). Since both devices exhibit almost the same increase in voltage due to the irradiation, it follows that the underlying (light-induced) changes must be occurring in layers and/or interfaces that are present in both devices and, therefore, are not related to the TPBi layer or the CBP/TPBi interface. This small ΔV may be the result of photodegradation of the ITO/MoO_3/CBP contact, which is known to happen.[16] The flow of current only (i.e., ⟨I only⟩) leads to an increase in V_d of ~0.63 V and 0.05 V in the devices with and without the TPBi layer, respectively. The larger ΔV value exhibited by the

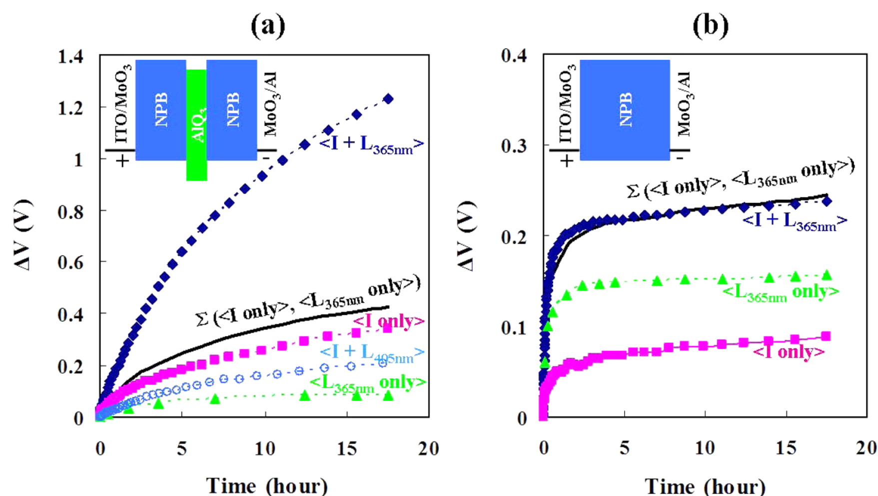

Figure 2. Changes in the V_d value at 20 mA/cm^2 in devices (a) with and (b) without the AlQ_3 layer, versus time, during which the devices are subjected to stress scenarios: ⟨I only⟩, ⟨$L_{365\ nm}$ only⟩, ⟨I + $L_{365\ nm}$⟩, and ⟨I + $L_{405\ nm}$⟩. The curve ∑(⟨I only⟩, ⟨$L_{365\ nm}$ only⟩) represents the algebraic sum of the ΔV in ⟨I only⟩ and ⟨$L_{365\ nm}$ only⟩.

device containing the TPBi layer may be attributed to hole accumulation at the CBP/TPBi interface,[3] because of the hole-blocking effect of TPBi.[18] Exposing the devices to irradiation and current flow simultaneously (i.e., ⟨I + $L_{365\ nm}$⟩) results in a faster increase in V_d in comparison to that induced by irradiation alone or current flow alone. What is most remarkable, however, is that the much faster increase in V_d in the device with the TPBi layer by this stress scenario ($\Delta V \approx$ 1.71 V) surpasses not only that in the device without the TPBi by the same scenario ($\Delta V \approx 0.14$ V) but also those produced by the separate exposure to irradiation or current flow (0.63 V and 0.08 V, respectively). For comparison, we include traces representing the algebraic sum of the ΔV values caused by ⟨I only⟩ and ⟨$L_{365\ nm}$ only⟩ (denoted by ∑(⟨I only⟩, ⟨$L_{365\ nm}$ only⟩)). As can be seen from Figure 1a, the measured ΔV values produced by the ⟨I + $L_{365\ nm}$⟩ scenario are much higher than the corresponding computed ∑(⟨I only⟩, ⟨$L_{365\ nm}$ only⟩) values, indicating that the effect of simultaneous exposure to light and current significantly surpasses the sum (or linear combination) of their individual contributions. This suggests that some interaction between the two stimuli (illumination and current flow) occurs, which leads to additional or faster degradation, hence the much faster voltage rise in this case. Since the distinguishing feature of ⟨I + $L_{365\ nm}$⟩, as compared to ⟨I only⟩ and ⟨$L_{365\ nm}$ only⟩, is the simultaneous presence of both positive polarons and CBP excitons, it is possible that the additional degradation in ⟨I + $L_{365\ nm}$⟩ in Figure 1a is due to interactions between positive polarons and CBP singlet excitons. Given that the concentration of excitons will be relatively uniform across the entire CBP layers (attenuation of 365 nm light in 40 nm of CBP is ∼5%[19]), whereas the concentration of positive polarons will generally be higher at the CBP/TPBi interface,[8] this interaction will most likely take place at the CBP/TPBi interface, rather than inside the CBP layer bulk or at the opposite TPBi/CBP interface. Since the concentration of excitons within the TPBi layer must be very small (TPBi absorption at 365 nm is negligible and energy transfer from CBP to TPBi is inefficient, because of the wider bandgap of TPBi), such interactions between excitons and polarons cannot be happening within the TPBi layer bulk. The results therefore suggest that interactions between CBP singlet excitons and CBP positive polarons at the CBP/TPBi interface must be behind the additional degradation. This is further verified from devices without TPBi, and thus no CBP/TPBi interface, in Figure 1b, where the ΔV value in the case of ⟨I + $L_{365\ nm}$⟩ is approximately equal to the sum of the individual effects of illumination and current (i.e., ∑(⟨I only⟩, ⟨$L_{365\ nm}$ only⟩)), indicating that the additional degradation processes are not significant when the interface is absent. To check if the second interface (i.e., the TPBi/CBP one) is contributing to this degradation behavior, we tested h-only devices that do not have the second CBP layer, and thus no TPBi/CBP interface [i.e., ITO/MoO_3(5 nm)/CBP(20 nm)/TPBi(5 nm)/MoO_3(5 nm)/Al(100 nm)], in order to compare their behavior to that of the devices in Figure 1a. The results show that these devices have essentially the same degradation behavior as that of the devices reported in Figure 1a, indicating that the second interface does not play a significant role in the observed degradation behavior. Therefore, the additional degradation in ⟨I + $L_{365\ nm}$⟩ in Figure 1a is primarily interfacial, and it is likely induced by interactions between CBP positive polarons and CBP singlet excitons at the CBP/TPBi interface. It should be noted that h-only devices subjected to ⟨I only⟩ and ⟨$L_{365\ nm}$ only⟩ in sequence (first ⟨I only⟩, then ⟨L only⟩ or first ⟨L only⟩, then ⟨I only⟩) show similar ΔV as in ∑(⟨I only⟩, ⟨ $L_{365\ nm}$ only⟩). This indicates that this interfacial degradation indeed occurs only when both excitons and polarons co-exist, as opposed, for example, to being the product of their individual effects in some particular sequence of events.

Finding that the CBP/TPBi interface degrades significantly when both positive polarons and excitons on CBP are present, we conduct similar studies on the NPB/AlQ_3 interface, utilizing NPB-based h-only devices that contain a thin AlQ_3 layer (∼5 nm thick), and thus an NPB/AlQ_3 interface, and others without the AlQ_3 layer for comparison. The device structure is ITO(120 nm)/MoO_3(5 nm)/NBP(20 nm)/AlQ_3(5 nm or 0 nm)/NPB(20 nm)/MoO_3(5 nm)/Al(100 nm), respectively. Figures 2a and 2b show the changes in V_d at 20 mA/cm^2 in devices with and without the AlQ_3 layer, respectively, as a function of time, under the same stress scenarios used above: ⟨I only⟩, ⟨$L_{365\ nm}$ only⟩, and ⟨I + $L_{365\ nm}$⟩. In addition, we use a fourth scenario, ⟨I + $L_{405\ nm}$⟩, in which the device is subjected to a current flow with a density of ∼20 mA/cm^2 and 405 nm irradiation of power density ∼0.5 mW/cm^2 simultaneously. Since the 405-nm

dx.doi.org/10.1021/am402537j | ACS Appl. Mater. Interfaces 2013, 5, 8733−8739

irradiation can excite AlQ_3 only,[15] whereas the 365 irradiation can excite both NPB and AlQ_3,[15,16] including this fourth scenario allows one to differentiate between the influence of NPB excitons versus AlQ_3 excitons in the degradation process. This approach was difficult to implement in the case of the CBP/TPBi devices, because of the significant overlap between CBP and TPBi optical absorption spectra, which makes it impossible to excite TPBi without exciting CBP.[9,15] The V_d value of the devices with and without the AlQ_3 layer (i.e., for the trends in Figures 2a and 2b, respectively) is ~8 V and ~2.4 V, respectively. As can be seen from the figures, the three stress scenarios ⟨$L_{365\ nm}$ only⟩, ⟨I only⟩, and ⟨I + $L_{365\ nm}$⟩ bring about changes in the V_d value of the devices with and without the AlQ_3 layer that very closely resemble, qualitatively, those in Figure 1. Here again, we see that the exposure to light alone (⟨$L_{365\ nm}$ only⟩) results in small and comparable changes in the V_d value ($\Delta V \approx 0.08$) in devices with and without the AlQ_3, indicating that these changes are not related to the AlQ_3 layer or the NPB/AlQ_3 interface. ⟨I only⟩ produces larger ΔV in the case of the device with the AlQ_3 layer, which, again, can be attributed to hole accumulation at the NPB/AlQ_3 interface.[3] Most importantly, again, the ΔV value caused by ⟨I + $L_{365\ nm}$⟩ surpasses the sum of the individual effects of illumination and current (i.e., $\sum$(⟨I only⟩, ⟨$L_{365\ nm}$ only⟩)) in the case of the device with the AlQ_3 layer (Figure 2a), but not in the case of the device without the AlQ_3 layer (Figure 2b). Such comparison again points to additional degradation mechanisms when the interface is present and is subjected to current and light simultaneously, revealing that interfacial degradation due to polaron−exciton interactions occurs in the case of NPB/AlQ_3 as well. More details of such degradation are revealed by utilizing 405-nm irradiation in Figure 2a, where the ΔV value caused by ⟨I + $L_{405\ nm}$⟩ is not as large as that caused by ⟨I + $L_{365\ nm}$⟩. [Note: we use the same power densities for both 365-nm and 405-nm irradiation. Therefore, the number of photons in the case of 405-nm irradiation is necessarily higher. Since AlQ_3 absorption at 405 nm is also higher,[15] the number of excitons on AlQ_3 in this scenario will be significantly higher.] Since only AlQ_3 excitons but no NPB excitons are created by the scenario ⟨I + $L_{405\ nm}$⟩, the results suggest that only NPB excitons play a significant role in the NPB/AlQ_3 interfacial degradation process. It should be pointed out that the ΔV value in the case of ⟨I + $L_{405\ nm}$⟩ is even slightly smaller than that in case of ⟨I only⟩, which may be due to the higher conductivity of AlQ_3 when under 405-nm irradiation,[9] which would reduce the concentration of polarons on the NPB side of the interface.

It is noteworthy to point out that we have also conducted similar studies utilizing electron-only devices to investigate if interactions between ETM negative polarons and excitons may have a similar effect on HTM/ETM interfaces. Preliminary results however show that subjecting the interfaces to electron current and light simultaneously leads to very little additional degradation. This may be due to the lower accumulation of electrons (relative to holes) at the HTM/ETM interfaces. It is also possible that interactions between ETM negative polarons and excitons do not cause the same degradation effect.

Since the above results show that interactions between positive polarons and singlet excitons on the HTM are responsible for HTM/ETM interfacial degradation, we would expect that reducing the exciton lifetime would reduce the interaction probability and thus slow down the degradation mechanism. To test for this, we study the effect of introducing a very thin layer of a narrower band-gap material, 4-(dicyano-methylene)-2-*tert*-butyl-6-(1,1,7,7-tetramethyljulolidyl-9-enyl)-4H-pyran (DCJTB), on the degradation behavior of the h-only CBP/TPBi devices. As the absorption spectrum of DCJTB and the emission spectrum of CBP significantly overlap, transfer of excitons from CBP to DCJTB via Forster process can be quite efficient, which would therefore reduce the lifetime of CBP singlet excitons. This effect is verified by fluorescence lifetime measurements. Figure 3 shows fluorescence versus time at 405

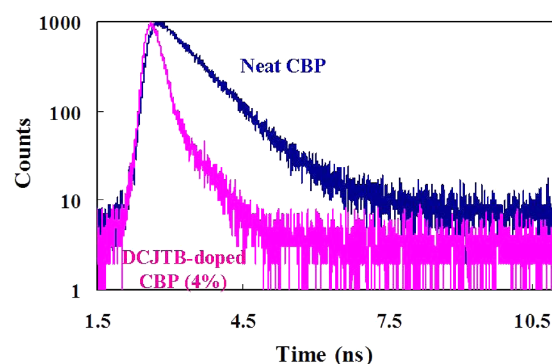

Figure 3. Time domain CBP fluorescence lifetime of 30-nm neat CBP and DCJTB-doped (4%) CBP films, excited by a 379-nm pulsed laser.

nm (i.e., from the relaxation of CBP singlet states) collected from a neat CBP film and a DCJTB-doped CBP film (doped at 4% by volume) excited by a 379-nm laser pulse (pulse width ≈ 71 ps, average power ≈ 5 mW). Clearly, the decay rate of CBP fluorescence becomes much faster in the presence of DCJTB, confirming the role of DCJTB in shortening the lifetime of CBP excitons.

Figures 4a−c show changes in V_d under the three stress scenarios ⟨I only⟩, ⟨$L_{365\ nm}$ only⟩, and ⟨I + $L_{365\ nm}$⟩ of CBP/TPBi h-only devices containing an ultrathin layer (~0.5 Å thick) of DCJTB, located at various distances from the CBP/TPBi interface. Figure 4d show the changes in V_d under the same conditions in the case of a control device without a DCJTB layer. The initial V_d values of these devices in Figures 4a, 4b, 4c, and 4d are 7.2, 8.5, 9.4, and 5.2 V, respectively. As can be seen from the figure, introducing the ultrathin layer of DCJTB at a distance of ~5 nm from the CBP/TPBi interface has almost no effect on the degradation behavior of the devices, evident in the close similarity between the voltage rise trends in Figures 4a and 4d. In contrast, as can be seen from Figure 4b, placing the layer much closer to the interface (only ~1 nm away) reduces the voltage rise caused by the ⟨I + $L_{365\ nm}$⟩ scenario significantly, pointing to a slowdown in the degradation process, in comparison to the control device. Quite remarkably, the voltage trend becomes very similar to the sum of the individual effects of illumination and current (i.e., $\sum$(⟨I only⟩, ⟨$L_{365\ nm}$ only⟩)), suggesting that the additional degradation by exciton−polaron interactions are indeed greatly suppressed in this case. Since the only difference between this device in Figure 4b and that in Figure 4a is the closer proximity of the DCJTB layer to the CBP/TPBi interface, which becomes comparable to the Förster radius in the case of Figure 4b, thus allowing efficient Förster energy transfer (FRET) from CBP excitons in the vicinity to the DCJTB layer, it is evident that reducing the lifetime of CBP excitons in the vicinity of the interface can indeed slow the degradation process. The fact that the DCJTB layer does not produce the same effect when the layer is 5 nm away from the interface further verifies that the

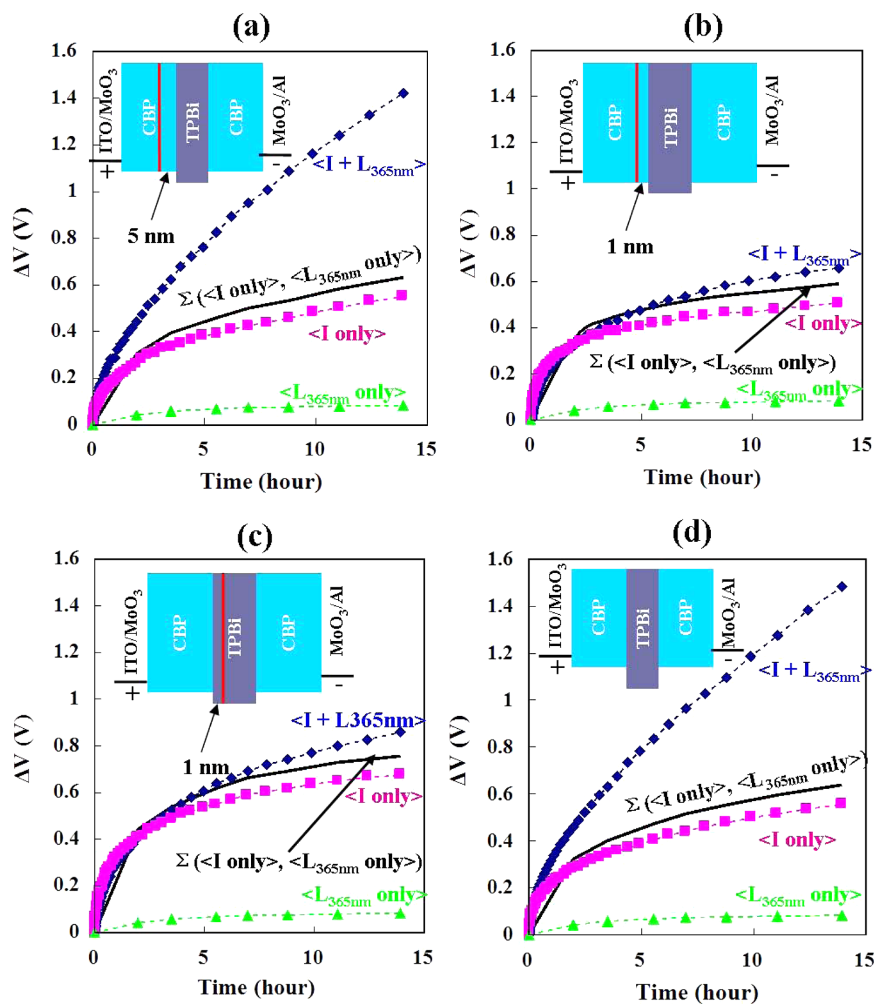

Figure 4. Changes in driving voltage (ΔV) at 20 mA/cm^2, versus time, in devices where (a) the DCJTB layer is in the CBP and 5 nm away from the CBP/TPBi interface, (b) the DCJTB layer is in the CBP and 1 nm away from the CBP/TPBi interface, (c) the DCJTB layer is in the TPBi and 1 nm away from the CBP/TPBi interface, and (d) no DCJTB layer is present during which the devices are subjected to the following scenarios: ⟨I only⟩, ⟨$L_{365\ nm}$ only⟩, and ⟨I + $L_{365\ nm}$⟩. The curve $\sum$(⟨I only⟩, ⟨$L_{365\ nm}$ only⟩) represents the algebraic sum of the ΔV values in ⟨I only⟩ and ⟨$L_{365\ nm}$ only⟩.

degradation process is entirely interfacial. Furthermore, the fact that the DCJTB layers affect the V_d stability differently in Figures 4b and 4a, even though they (i.e., the DCJTB layers) fall on the conduction path of holes from the ITO/MoO_3 contact to the CBP/TPBi interface in both cases rules out the possibility that the effect may primarily be the result of a change in the polaron concentration in the CBP layer or at the CBP/TPBi due to hole trapping on DCJTB. This is further verified from tests on the device where the DCJTB layer is located in the TPBi layer and therefore is "downstream" of the hole conduction path, relative to the CBP/TPBi interface. It can be clearly seen from Figure 4c that, in this case, the DCJTB brings about almost the same effect on the V_d stability as that in the case of Figure 4b. Since one can expect energy transfer from CBP excitons at the interface to the DCJTB layer via the Förster process to be similar in the case of Figures 4b and 4c (both have DCJTB located at the same distance from the interface), whereas polaron redistribution due to the presence of the DCJTB can be expected to be different in the two cases, the results convincingly prove that the primary role of DCJTB in enhancing the stability under the ⟨I + $L_{365\ nm}$⟩ scenario stems from its role in reducing the lifetime of CBP excitons.

The above results clearly reveal that HTM/ETM interfaces degrade rapidly when both HTM positive polarons and HTM singlet excitons are present simultaneously in their vicinity, resulting in a deterioration in conduction across the interface. This degradation mechanism involves some interaction between the two species (i.e., HTM positive polarons and HTM singlet excitons) and can be slowed if the exciton lifetime is made shorter. Although the observations are obtained from h-only test devices, the close similarity between the interface conditions in these test devices and actual OLEDs suggests that the same phenomenon likely happens at interfaces of actual OLEDs. To further investigate this, we study the V_d stability of archetypical OLEDs containing CBP/TPBi and NPB/AlQ_3 interfaces. In some of these devices, we introduce a small amount of 3,4,9,10-perylenetetracarboxylic-bis-benzimidazole (PTCBI), to serve as an exciton quencher, in a portion of the ETM, thereby testing the effect of reducing exciton lifetime (and concentration) on the device performance. We first fabricate and test changes in V_d versus time of continuous electrical driving at 20 mA/cm^2 in two CBP/TPBi-based OLEDs of structures ITO(120 nm)/MoO_3(5 nm)/CBP(40 nm)/TPBi(30 nm)/LiF(1 nm)/Al(100 nm) and ITO(120 nm)/MoO_3(5 nm)/CBP(40 nm)/TPBi(5 nm)/

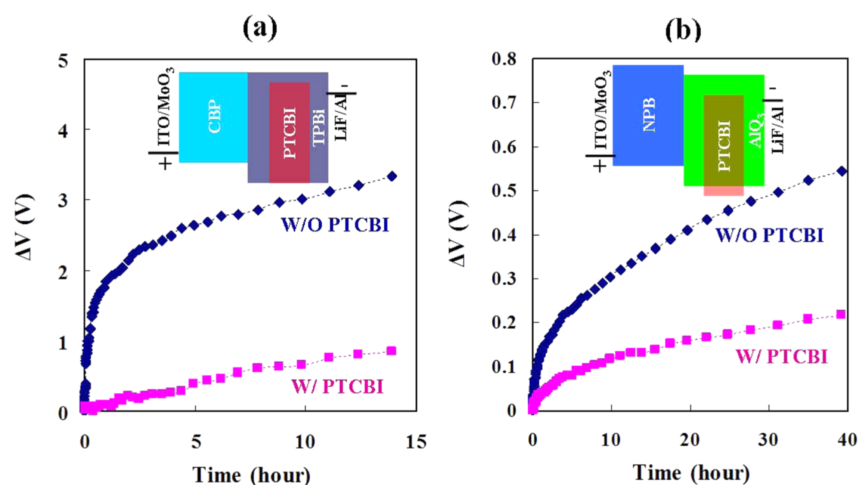

Figure 5. Change in driving voltage (ΔV) at a current of density 20 mA/cm^2 in (a) CBP/TPBi-based and (b) NPB/AlQ$_3$-based OLEDs versus time of continuous electrical driving.

TPBi:PTCBI(2%)(20 nm)/TPBi(5 nm)/LiF(1 nm)/Al(100 nm). The PTCBI is doped only in the middle region of the TPBi layer to avoid altering the chemical composition of the CBP/TPBi interface. The initial V_d value of the devices with and without PTCBI is 10.2 V and 9.1 V, respectively. Under this electrical driving, the device without the PTCBI produces blue EL from CBP with a brightness of 50 cd/m^2, whereas, as expected, the device with the PTCBI shows no detectable EL, because of the efficient quenching of CBP excitons by the PTCBI. We can expect the concentration of positive polarons in the CBP layer in the vicinity of the CBP/TPBi interface to be comparable in both devices (or slightly higher in the case of the device with the PTCBi-doped region, because of a possible decrease in electron transport across the TPBi layer, due to some electron trapping on PTCBI, as the somewhat higher V_d value suggests). At the same time, we can expect the lifetime of CBP excitons to be much shorter in the case of the device with the PTCBi, because of the quenching effect by the PTCBi. We would therefore expect the interfacial degradation process to be slower in the case of the device with the PTCBi due to a reduction in exciton−polaron interactions and thus expect to see higher voltage stability, in comparison to the control device (i.e., without PTCBI). Figure 5a shows the changes in V_d versus time of continuous electrical driving at 20 mA/cm^2 of these devices. As the figure shows, the device without the PTCBI shows an increase in voltage of 3.3 V, whereas the device with the PTCBI shows an increase in voltage of only 0.8 V, confirming the occurrence of CBP/TPBi interfacial degradation in OLEDs due to polaron−exciton interactions. It should be noted that tests on CBP/TPBi-based OLEDs that contain phosphorescent dopants such as fac-tris(2-phenylpyridyl)-iridium(III) (Irppy$_3$) show the same results. We also have carried out similar studies on NPB/AlQ$_3$-based OLEDs. Figure 5b shows the changes in V_d versus time of continuous electrical driving at 20 mA/cm^2 of these devices. The initial V_d values of the devices with and without the PTCBI are 7.2 and 5.4 V, respectively. The device without PTCBI produces green EL from AlQ$_3$ with a brightness of 450 cd/m^2, whereas the device with PTCBI produces only very weak EL (a brightness of ~4 cd/m^2). Again, as the figure shows, the device with the PTCBI shows a smaller ΔV than that without the PTCBI, indicating a slower interfacial degradation at the NPB/AlQ$_3$ interface. These results show that the degradation of HTM/ETM interfaces indeed occurs in OLEDs and is behind the fast increase in V_d in these devices with time; the latter being a behavior that is widely observed in OLEDs in general.

Although this study has focused on HTM/ETM interfaces, it is reasonable to expect that this interfacial degradation phenomenon will not be limited to these specific interfaces, but rather could affect all organic/organic interfaces in general whenever both positive polarons and excitons are present in their vicinity. For example, in the case of multilayered OLEDs, a buildup of positive polarons can occur at other device interfaces such as at interfaces between hole transport layers with different highest occupied molecular orbital energy levels. In addition, excitons may also be present at these interfaces, because of diffusion from the electron−hole recombination zone. Therefore, such interfaces may be similarly susceptible to interfacial degradation, as a result of polaron−exciton interactions.

4. CONCLUSIONS

In conclusion, we determined that the hole transport material/electron transport material (HTM/ETM) interfaces commonly used in organic light-emitting devices (OLEDs) degrade rapidly, because of an interaction between HTM positive polarons and HTM singlet excitons. The phenomenon results in a deterioration in conduction across the interface, and contributes to the commonly observed increase in OLED driving voltage with electrical driving time. This interfacial degradation can be slowed if the exciton lifetime becomes shorter. The findings uncover a new degradation mechanism that is interfacial in nature, which affects organic/organic interfaces in OLEDs and contributes to their limited electroluminescence (EL) stability, and shed light on approaches for reducing degradation. Although this study has focused on OLEDs, we can expect the same degradation mechanism to affect organic/organic interfaces in other organic optoelectronic devices where both excitons and polarons are present in high concentrations, such as in organic solar cells or photodetectors.

■ AUTHOR INFORMATION

Corresponding Author

*E-mail: h2aziz@uwaterloo.ca.

Notes

The authors declare no competing financial interest.

■ ACKNOWLEDGMENTS

Financial support to this work by Teledyne-DALSA and the Natural Science and Engineering Research Council of Canada (NSERC) is gratefully acknowledged.

■ REFERENCES

(1) Helander, M. G.; Wang, Z. B.; Qiu, J.; Greiner, M. T.; Puzzo, D. P.; Liu, Z. W.; Lu, Z. H. *Science* **2011**, *332*, 944.

(2) Aziz, H.; Popovic, Z. D. *Chem. Mater.* **2004**, *16*, 4522.

(3) Aziz, H.; Popovic, Z. D.; Hu, N.-X.; Hor, A.-M.; Xu, G. *Science* **1999**, *283*, 1900.

(4) Luo, Y.; Aziz, H.; Xu, G.; Popovic, Z. D. *Chem. Mater.* **2007**, *19*, 2079−2083.

(5) So, F.; Kondakov, D. Y. *Adv. Funct. Mater.* **2010**, *22*, 3762−3777.

(6) Kondakov, D. Y. *J. Appl. Phys.* **2008**, *104*, 084520.

(7) Kondakov, D. Y.; Lenhart, W. C.; Nichols, W. F. *J. Appl. Phys.* **2007**, *101*, 024512.

(8) Giebink, N. C.; D'Andrade, B. W.; Weaver, M. S.; Mackenzie, P. B.; Brown, J. J.; Thompson, M. E.; Forrest, S. R. *J. Appl. Phys.* **2008**, *103*, 044509.

(9) Giebink, N. C.; D'Andrade, B. W.; Weaver, M. S.; Brown, J. J.; Forrest, S. R. *J. Appl. Phys.* **2009**, *105*, 124514.

(10) Scholz, S.; Meerheim, R.; Walzer, K.; Leo, K. *Proc. SPIE* **2008**, *6999*, 69991B.

(11) Siboni, H.; Aziz, H. *Appl. Phys. Lett.* **2012**, *101*, 173502.

(12) Siboni, H.; Aziz, H. *Org. Electron.* **2011**, *12*, 2056−2060.

(13) Siboni, H.; Luo, Y.; Aziz, H. *J. Appl. Phys.* **2011**, *109*, 044501.

(14) Wang, Q.; Luo, Y.; Aziz, H. *Appl. Phys. Lett.* **2010**, *97*, 063309.

(15) Wang, Q.; Williams, G.; Tsui, T.; Aziz, H. *J. Appl. Phys.* **2012**, *112*, 064502.

(16) Wang, Q.; Williams, G.; Aziz, H. *Org. Electron.* **2012**, *13*, 2075−2082.

(17) Williams, G.; Wang, Q.; Aziz, H. *Adv. Funct. Mater.* **2013**, *23*, 2239−2247.

(18) Baek, H.; Lee, C. *J. Appl. Phys.* **2008**, *103*, 054510.

(19) Holzer, W.; Penzkofer, A.; Tsuboi, T. *Chem. Phys.* **2005**, *308*, 93−102.